JACS
JOURNAL OF THE AMERICAN CHEMICAL SOCIETY

Article

pubs.acs.org/JACS

Determination of Ion Atmosphere Effects on the Nucleic Acid Electrostatic Potential and Ligand Association Using AH^+·C Wobble Formation in Double-Stranded DNA

Benjamin E. Allred,[†] Magdalena Gebala,[†] and Daniel Herschlag*[,†,‡,§]

[†]Department of Biochemistry, Stanford University, Stanford, California 94305, United States
[‡]Department of Chemistry, Stanford University, Stanford, California 94305, United States
[§]ChEM-H Institute, Stanford University, Stanford, California 94305, United States

Supporting Information

ABSTRACT: The high charge density of nucleic acids and resulting ion atmosphere profoundly influence the conformational landscape of RNA and DNA and their association with small molecules and proteins. Electrostatic theories have been applied to quantitatively model the electrostatic potential surrounding nucleic acids and the effects of the surrounding ion atmosphere, but experimental measures of the potential and tests of these models have often been complicated by conformational changes and multisite binding equilibria, among other factors. We sought a simple system to further test the basic predictions from electrostatics theory and to measure the energetic consequences of the nucleic acid electrostatic field. We turned to a DNA system developed by Bevilacqua and co-workers that involves a proton as a ligand whose binding is accompanied by formation of an internal AH^+·C wobble pair [Siegfried, N. A., et al. *Biochemistry*, **2010**, *49*, 3225]. Consistent with predictions from polyelectrolyte models, we observed logarithmic dependences of proton affinity versus salt concentration of −0.96 ± 0.03 and −0.52 ± 0.01 with monovalent and divalent cations, respectively, and these results help clarify prior results that appeared to conflict with these fundamental models. Strikingly, quantitation of the ion atmosphere content indicates that divalent cations are preferentially lost over monovalent cations upon A·C protonation, providing experimental indication of the preferential localization of more highly charged cations to the inner shell of the ion atmosphere. The internal AH^+·C wobble system further allowed us to parse energetic contributions and extract estimates for the electrostatic potential at the position of protonation. The results give a potential near the DNA surface at 20 mM Mg^{2+} that is much less substantial than at 20 mM K^+ (−120 mV vs −210 mV). These values and difference are similar to predictions from theory, and the potential is substantially reduced at higher salt, also as predicted; however, even at 1 M K^+ the potential remains substantial, counter to common assumptions. The A·C protonation module allows extraction of new properties of the ion atmosphere and provides an electrostatic meter that will allow local electrostatic potential and energetics to be measured within nucleic acids and their complexes with proteins.

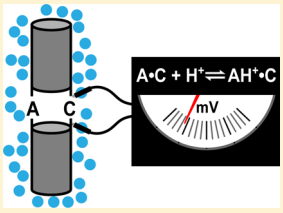

INTRODUCTION

The biological functions of nucleic acids rely on their association with protein and small molecule ligands (Figure 1A). Each binding event comprises forming and breaking multiple interactions, including hydrogen bonds, stacking, van der Waals interactions, and ion pairs. These interactions are also typical of ligands associating with proteins, but associations with nucleic acids involve additional factors. The high charge densities of nucleic acids generate large electrostatic potentials that attract oppositely charged ligands. These high charge densities also result in the formation of the ion atmosphere—a sheath of mobile ions that surrounds DNA, RNA, and other polyelectrolytes (Figure 1B) —that responds to and mitigates electrostatic interactions.[1−3] Thus, understanding nucleic acid-ligand associations necessitates accounting for the nucleic acid electrostatic potential, how the ion atmosphere mitigates this potential, and how the ion atmosphere changes upon ligand association.[4−6]

Given the complex and dynamic nature of the ion atmosphere, understanding its properties and effects requires synergy between theory and experiment. One of the first theoretical approaches developed for polyelectrolyte electrostatics was Manning's counterion condensation theory, which used a linear charge model to predict the presence and properties of the ion atmosphere.[6,7] Record applied this model to predict and interpret the effects of the ion atmosphere on ligand association.[5,8] Subsequently, the Poisson−Boltzmann equation (PB), a general quantitative model of electrostatic potentials in ionic solutions, was applied to simplified and atomic-level models of nucleic acids,[9−12] and the development of suitable resources for numerical solutions and a convenient web-based server have led to widespread use of this model to predict and visualize the electrostatic properties of biomolecules.[13,14]

Association equilibria of charged ligands to nucleic acids have been observed to be strongly sensitive to solution ionic conditions. For simple ligands binding to double-stranded DNA (dsDNA), the counterion condensation and PB models

Received: February 21, 2017
Published: May 10, 2017

DOI: 10.1021/jacs.7b01830
J. Am. Chem. Soc. 2017, 139, 7540−7548

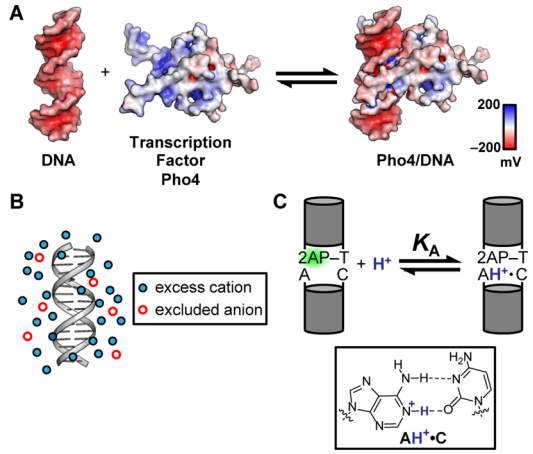

Figure 1. Electrostatic interactions underlying nucleic acid ligand binding. (A) An example of a functional nucleic acid ligand complex, the transcriptional factor Pho4 binding to DNA (PDB 1A0A).[45] The surface potential at 0.1 M monovalent salt, calculated using the APBS server,[13,46,47] is illustrated with the red/blue color scale. (B) Schematic representation of the ion atmosphere surrounding a nucleic acid. Excess cations and excluded anions, relative to bulk (not shown), sum to give an overall charge neutral system (i.e., the circles represent the number of ions per DNA in excess of the background concentration).[48,49] (C) Model system ($24bp^{AC}$) used in this study. In the middle of a 24-bp duplex DNA (gray cylinders), an A·C mismatch binds a proton to form an AH^+·C wobble pair (inset) with the proton association constant, K_A. The fluorescence of an adjacent 2-aminopurine (2AP) is sensitive to the protonation state of the A·C pair, with greater fluorescence in the deprotonated state (green), and is used to readout the equilibrium.

predict that the log of the association constant varies with the log of monovalent cation concentrations with a slope of −0.8 to −1 per positive charge of the ligand, and a slope of 2-fold lower value is predicted for the dependence on divalent cation concentration.[5,6,8,15,16] A number of experiments in which association constants for Mg^{2+}, polyamines, and oligopeptide ligands were determined as a function of salt concentration support these predictions.[5,8,17−29] However, the systems used, in particular the flexibility of single-stranded nucleic acids and oligopeptides, can involve conformational changes coupled to binding that could alter the ion dependence of association and could render inadequate the simplified rigid, charged rods models that were used in analysis. Also, these ligands bind nucleic acids nonspecifically and modeling their binding required fits to multisite binding equilibria and assumptions about the size of the binding site and how binding of successive ligands are affected by the previously bound ligands. In examining protein association to nucleic acids, ad hoc treatment of protein ionization states and definitions of which charged residues interact and which do not have been used,[16,30−37] and these simplifications have persisted in the literature despite the inadequacies of this analysis having been identified.[38−40] In addition, several reported salt dependences do not agree with predictions from PB theory and alternative or ad hoc explanations have been provided, stressing the need for systematic analysis with a simple model system.[30−33,41,42]

To address the above-noted uncertainties and to provide a foundation from which to systematically build toward a quantitative understanding of complex protein-nucleic acid systems, we turned to a dsDNA system developed by Bevilacqua and co-workers that involves a proton as a ligand that specifically binds to one well-defined site—an A·C mismatch to form an AH^+·C wobble—and is expected to involve only local conformational rearrangement (Figure 1C).[42−44] We observed the salt dependence of association expected from polyelectrolyte models, providing strong support for overarching aspects of the counterion condensation and PB formulations of the ion atmosphere and its effects. Further, thermodynamic reference states for this system allowed us to construct a thermodynamic cycle to estimate the electrostatic potential of the dsDNA and its variation with salt identity and concentration. Our results provide a foundation and tool for determining and dissecting energetics and electrostatic potentials in more complex protein-nucleic acid systems.

MATERIALS AND METHODS

DNA Sequences. The two strands of the $24bp^{AC}$ construct were $_{5'}$GGT GAC GAC TT2 ATC ACT GGG CGG$_{3'}$ and $_{5'}$CCG CCC AGT GAC TAA GTC GTC ACC$_{3'}$, where 2 indicates 2-aminopurine. The secondary structure of $24bp^{AC}$, a fully base-paired control, $24bp^{AT}$, and the construct used for ion counting are shown in Figure S1.

Preparation of DNA Samples. Chemically synthesized oligonucleotides (Integrated DNA Technologies, USA) were purified by reverse phase HPLC (XBridge Oligonucleotide BEH C18 Prep Column, Waters, MA). Following desalting in Amicon Ultra-3K filters (Millipore, MA), the DNA was annealed by mixing the 2AP containing strand with 1.2 equiv of the complementary strand in 5 mM KCl and warming to 40 °C for 5 min. The solution was unbuffered to not perturb the pH in the proton binding assays. Nondenaturing PAGE showed no remaining unannealed 2AP strand (<0.1%), and control experiments showed single-stranded 2AP does not contribute to a pH-dependent fluorescence change in the binding assays (Figure S2). Following hybridization, equilibration into 5 mM KCl was carried out with eight rounds of buffer exchange using Amicon Ultracel-30K filters (Millipore, MA), as reported previously.[48,49]

Proton Binding Assays. Proton binding assays were conducted by measuring the 2AP fluorescence in pH-buffered solutions at the indicated salt concentration. An array of 44 buffer solutions was used for each affinity measurement. Individual solutions were made by dissolving potassium acetate or one of the free acids of MES, MOPS, HEPES, TAPS, CHES, and CAPS. The pH was set by addition of concentrated HCl to the potassium acetate or a solution of KOH to the other buffers. The pH was measured at 5 mM buffer and 10 mM K^+ and calculated for other ionic conditions using the Davies equation, an empirical extension of the Debye−Huckel equation (eq 1),

$$\log \gamma_i = -Az_i^2\left(\frac{\sqrt{I}}{1+\sqrt{I}} - 0.3I\right) \quad (1)$$

where γ_i is the activity coefficient of a species, A is a constant equal to 0.5 $M^{-1/2}$, z_i is the charge of that species, and I is the ionic strength of the solution.[50] The accuracy of this calculation was confirmed with pK_a measurements of standard cationic and anionic dyes (*p*-nitrophenol and neutral red, respectively) with an array of buffers at several salt concentrations across the range used for the experiments herein. The observed pK_a values were within 0.1 of the pK_a values calculated from literature values for salt concentrations from 0.01 to 1 M (Table S1). Buffer solutions were stored at −20 °C to reduce CO_2 absorption, and the pH of the buffer solutions was measured periodically to correct for changes from CO_2 absorption, which occurred predominantly in the high pH buffers. The free salt concentrations reported are the sum of the added salt solution, the free salt in the DNA solutions, and the K^+ in the buffer stock solutions. pH values were maintained above pH 5.0 to minimize DNA damage via deamination, and the absence of circular dichroism (CD) or fluorescence over time or at the lowest pH values suggested the absence of significant DNA damage at low pH.

Fluorescence (ex. 340 nm, em. 371 nm) was measured at 25 °C by 90° detection in quartz cells using a Fluorolog-3 instrument (Horiba, USA) or by top detection in a 96-well plate using Infinite M200 pro plate reader (Tecan, Switzerland). Measurements with the individual cell and

DOI: 10.1021/jacs.7b01830
J. Am. Chem. Soc. 2017, 139, 7540−7548

plate formats gave the same equilibrium constants, within error. DNA concentrations between 1 and 10 μM were used and gave a greater than 2-fold fluorescence change between the protonated and deprotonated states with a high signal-to-noise ratio. Representative titrations are shown in Figure S3. A construct with an AT pair in place of the A·C mismatch (24bp^{AT}) and a single stranded oligonucleotide with 2AP gave no pH-dependent fluorescent signal (Figure S2).

The proton association constant, K_A, was derived from fitting the observed pH-dependent fluorescence change with a single proton binding model for 24bp^{AC} (eq 2):

$$F_{tot} = F_{AH^+\cdot C} + \frac{F_{A\cdot C} - F_{AH^+\cdot C}}{1 + 10^{(\log K_A - pH)}} \quad (2)$$

In eq 2 F_{tot} is the total fluorescence and $F_{AH+\cdot C}$ and $F_{A\cdot C}$ are the fluorescence of the AH$^+$·C wobble pair and the A·C mismatch, respectively. Representative data and fits are shown in Figure S3. Individual log K_A values are reported in Tables S2–S5. Independent log K_A measurements were plotted versus the log of the cation concentration (and salt activity for monovalent cations) and fit with a straight line. The same proton affinities were observed in experiments varying DNA concentration 3-fold, indicating that the absence of an effect at low Mg^{2+} is not the result of a titration effect and insufficient total Mg^{2+}. The ion-counting results also support the lack of titration effect at 0.1–1 mM Mg^{2+}, in that a solution of 3 μM DNA "binds" at most 6 μM Mg^{2+}, and the difference between total Mg^{2+} and free Mg^{2+} is less than 10%.

Buffer Equilibration and Ion Counting. Buffer-equilibration and ion counting were carried out as reported previously.[48,49] Briefly, DNA was purified as described above, followed by hybridization in 160 mM K^+ at the pH of the experiment. Successive buffer exchanges (eight rounds) with the appropriate ionic conditions and pH were carried out at 4 °C using Amicon Ultra-30K filters (Millipore, MA). Aliquots of the DNA-containing sample, the flow-through, and the buffer were diluted into 5 mL of 50 mM ammonium acetate (pH 5.0). Dilution factors were determined so that the phosphorus (from DNA), potassium, and magnesium concentrations were within the linear range of ICP-OES detection. The concentrations in each solution were determined simultaneously using an ICAP 6300 Duo View Spectrometer (Thermo Scientific, USA) calibrated with ICP standards (Spex Certiprep, USA). The number of cations associated with a DNA was calculated using eq 3,

$$\text{number of cations} = \frac{C_{ion}^{DNA} - C_{ion}^{buffer}}{C_{DNA}} \quad (3)$$

where C_{ion} is the cation concentration of the DNA-sample and buffer, respectively, and C_{DNA} is the DNA concentration. The number of anions excluded by the DNA was not quantified because Cl^- concentration is not measurable in this experimental system.

Poisson–Boltzmann Calculations. A molecular model of fully base-paired 24bp^{AT}—with an AT pair in place of the A·C mismatch of 24bp^{AC}—was constructed using the generic B-form helix and the corresponding sequence in the 3DNA web server.[51] The duplex is shown in Figure S1. Charges were assigned with the PDB 2PQR routine using the CHARMM parameter set,[46,47] and protonation was modeled by adding charge of +1 to N1 of adenine. Calculations using a dsDNA in which the AT pair is replaced with an AH$^+$·C wobble from crystal structure PDB 1D99[52] give the same K^+ concentration dependence of association (slope = −0.90, see Figure 2B) as the fully base-paired helix. The PB equation was numerically solved to give electrostatic energies using the Adaptive Poisson–Boltzmann Solver (APBS) on a 482 × 482 × 562 Å grid with a 2.5 Å grid spacing and ion size equal to 2 Å. The external dielectric was set at 78.54, typical of water at 25 °C, and the internal dielectric was 2.0. Increasing the grid size by 50% or decreasing the spacing to 1.5 Å gave results within 1%.

The number of ions associated with the DNA was computed by integrating the excess ion density using eq 4,

$$n_i = \rho_{b,i} \int (\lambda(r) e^{-z_i e \varphi(r)/kT} - 1)\, dr \quad (4)$$

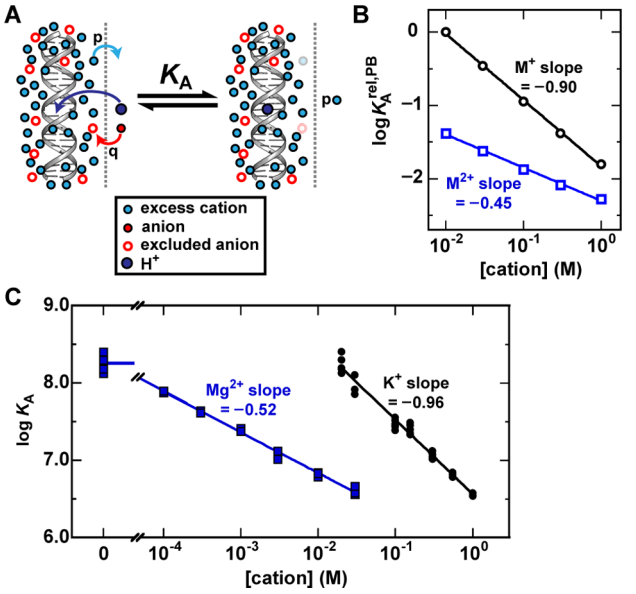

Figure 2. Effects of monovalent cations on proton association with 24bp^{AC}. (A) Thermodynamic model of proton binding to 24bp^{AC} and the accompanying reorganization of the ion atmosphere. The dashed line schematically represents the boundary between the ion atmosphere and bulk solution. The ensemble average of the change in the ion atmosphere upon proton binding is represented by the binding of **q** anions and the release of **p** cations. Thus, relative to the proton dissociated state, the ion atmosphere of the proton bound state thus has **p** fewer excess cations and **q** fewer excluded anions (see eqs 5 and 6). (B) Poisson–Boltzmann predicted effects of monovalent and divalent cations on proton association for 24bp^{AC}. Values are relative to the proton affinity in 10 mM monovalent cation ($K_A^{rel,PB}$). (C) Observed dependence of proton association for 24bp^{AC} on K^+ and Mg^{2+} concentration at 25 °C. Points represent independent measurements and the line is the best fit. (Mg^{2+} concentration was varied with a background of 20 mM K^+.) Individual log K_A values and errors are given in Tables S2 and S5. Linear parameters and errors are given in Table S6 and S7.

where $\rho_{b,i}$ is the bulk ion concentration, $\lambda(r)$ defines the region in the grid that is accessible to ions ($\lambda(r) = 1$ for accessible regions and $\lambda(r) = 0$ for the solvent-excluded region—i.e., inside the macromolecule), e is the elementary charge, $\varphi(r)$ is the electrostatic potential, k is the Boltzmann constant, and T is the temperature.[12,38] The dependence of log K_A on salt concentration for the sphere models was calculated as describe in the Supporting Information Methods.

BACKGROUND

The complex, dynamic nature of the ion atmosphere has rendered it difficult to study by experimental methods.[3,48] Therefore, our perspective on the contributing forces and components of the ion atmosphere has depended extensively on theory and computational models. Among electrostatic theories, PB theory provides a simplified, physics-based formulation of the ion atmosphere—i.e., a mean-field approximation representing ions as distributions rather than discrete point charges—that in many cases makes predictions that are consistent with experiment.[15,49,40,53] Below we present core electrostatic and ion atmosphere concepts that are tested and built upon in the experimental sections. We use PB theory for its simplicity, tractability, and general agreement with observations.

In PB theory, association of a charged ligand is predicted to be strongly dependent on salt concentration. These salt effects depend on how surrounding ions redistribute upon ligand

DOI: 10.1021/jacs.7b01830
J. Am. Chem. Soc. 2017, 139, 7540–7548

binding, and the nature of this redistribution in turn depends on the charge density of the system (Figure S4). For low charge density molecules, for which the surrounding electrostatic potential is less than thermal energy, the degree of attraction of cations and repulsion of anions are similar, resulting in a shallow dependence of the equilibrium constant on salt concentration. These dependences are typically modeled by the Debye−Huckel equation, a linearized simplification of PB theory.[54]

For polyelectrolytes, like DNA and RNA, the situation is different. PB theory predicts that a molecule with high negative charge density strongly attracts opposite-charged ions and repels fewer like-charged ions (Figure 1B; Figure S4B).[55−57,48] This predicted asymmetry has been demonstrated by ion-counting methods that quantify the large excess of cations and smaller exclusion of anions in the ion atmosphere of DNA.[48,49] With a dominant accumulation of cations in the ion atmosphere, nucleic acid systems are predicted to respond to association of a positively charged ligand, such as the proton depicted in Figure 2A, by predominantly releasing cations ($\mathbf{p} > \mathbf{q}$, where $\mathbf{p}$ is the number of excess cations released and $\mathbf{q}$ is the number of anions bound per molecule).[38,58] Thus, as salt concentration is increased, the cation concentration would have a larger effect than the opposing effect of the anion concentration and would substantially decrease the equilibrium constant (Figure S4C). The change in the log of the association constant with the log of monovalent cation concentration is related to the change in the ion atmosphere composition as shown in eq 5, below, where p and q are defined above.[38,58]

$$-\frac{\partial \log K}{\partial \log[MX]} = p - q \tag{5}$$

At the high extreme of charge density, the slope reaches a limit of −1 per ligand charge, thereby maintaining the charge neutrality of the system upon ligand association exclusively by release of a cation (Figure S4D). With divalent cations, charge neutrality is maintained by releasing fewer cations, and the slopes are predicted to reach a limit of −0.5, one-half of that in monovalent cations (Figure S4E and F). With an asymmetric salt, such as $MgCl_2$, the slope is related to the number of cations released and anions bound as shown in eq 6.[38,59]

$$-\frac{\partial \log K}{\partial \log[MX_2]} = p - 2q \tag{6}$$

The nucleic acid charge density and the ion concentration and identity together determine the ion atmosphere composition, and these factors determine the electrostatic potential at each distance from the nucleic acid (Figure S5A and B). This potential, in turn dictates the strength of attraction of an oppositely charged ligand (Figure S5C and D) where for a simple, singly charged ligand (L^+) the attraction is equivalent to the work required to move the ligand from a position near the helix with an electrostatic potential ψ_x to a position infinitely distant from the helix, with the potential ψ_∞ defined as zero. Per mole of ligand, the attraction from the electrostatic potential is defined in terms of a free energy, $\Delta G^{\psi x}_{L+}$ (eq 7), where N_A is Avogadro's number and e is the elementary charge.

$$\Delta G^{\psi x}_{L+} = -N_A \cdot e \cdot (\psi_x - \psi_\infty) = -N_A \cdot e \cdot \psi_x \tag{7}$$

PB theory predicts electrostatic potentials near to a DNA helix on the order of −200 to −300 mV (Figure S5E and F).[9,11] This value is expected to be a rough estimate as surface steric effects and discrete solvation and ion effects, which are difficult to model, are not accounted for in the mean field approximation of PB. Nevertheless, PB provides a benchmark for the experimentally derived estimate of the electrostatic potential provided herein from proton affinity measurements and thermodynamic cycles (Figure 3 below).

RESULTS AND DISCUSSION

The Effect of the Ion Atmosphere on Ligand Association. To isolate the influence of the ion atmosphere on ligand association, we used a model system with an A·C mismatch in the center of a 24 bp DNA duplex ($24bp^{AC}$, Figure 1C). The duplex provides an ion atmosphere without complications from specific metal ion binding sites or a broad and varying ensemble of conformational states. The A·C mismatch provides a binding site for arguably the simplest ligand possible, a proton, that when bound to N1 of the adenine stabilizes formation of a wobble pair with the cytosine on the opposite strand (Figure 1C, inset). The fluorescence of the adjacent 2-aminopurine (2AP) is sensitive to the formation of the wobble pair and is used to quantify the proton association constant K_A (Figure 1C).[43] Circular dichroism (CD) of the unprotonated and protonated duplex suggests that the transition results in minimal conformational perturbations, consistent with previous observations that perturbations arising from mismatches and wobble pairs are highly localized (Figure S6).[60−62]

For the model helix system, PB predicts that the proton association constant (K_A) decreases with a slope of −0.90 with added monovalent cations (Figure 2B), corresponding to an average release of 0.95 cations ($\mathbf{p}$) and accumulation of 0.05 anions ($\mathbf{q}$) per binding event (Figure 2A and eq 5). With added divalent cations, a slope of −0.45 is predicted, as fewer cations need to be released to maintain charge neutrality, corresponding to 0.49 divalent cations released and 0.02 anions accumulated upon ligand binding per DNA (Figure 2B and eq 6).

Figure 2C shows how the proton association constant of the model system changes with increasing concentrations of K^+. The observed slope was −0.96 ± 0.03, and while the PB prediction is outside the fitting error, the difference is small and provides general support for the PB model. Carrying out the analogous experiment with Mg^{2+} also gave the expected shallower dependence, with a slope of −0.52 ± 0.01. The proton affinity (K_A) was lower in Mg^{2+} than in K^+ for the overlapping salt concentrations in Figure 2C, as predicted for stronger shielding of the DNA negative charge by Mg^{2+} than K^+.[59,63] For example, at 30 mM K^+ or Mg^{2+}, the ratio of observed K_A values is 23-fold, similar to the value of 15-fold predicted by PB calculations (Figure 2B).

If the observed salt effects arise from long-range interactions between mobile ions and the DNA, as opposed to direct contact interactions, it is expected that these effects will be independent of ion identity.[64] We tested this expectation with Li^+ and Cs^+ for the K^+ effect and with Ba^{2+} for the Mg^{2+} effect and observed consistent effects for cations of the same valence (Figure S7). These results support that proton association with $24bp^{AC}$ is minimally influenced by specific metal ion binding and that this system is suitable for testing ion atmosphere effects.

Overall, our results agree closely with predictions from simple polyelectrolyte theory. However, prior studies suggested a slope of −0.34 for log K_A versus log $[K^+]$ for protonation of an A·C mismatch in a DNA hairpin,[42] considerably different than the slope of −0.96 observed herein and inconsistent with predictions from PB and other electrostatic theories. As the prior experiments involved NMR titrations, they required high nucleic

DOI: 10.1021/jacs.7b01830
J. Am. Chem. Soc. 2017, 139, 7540−7548

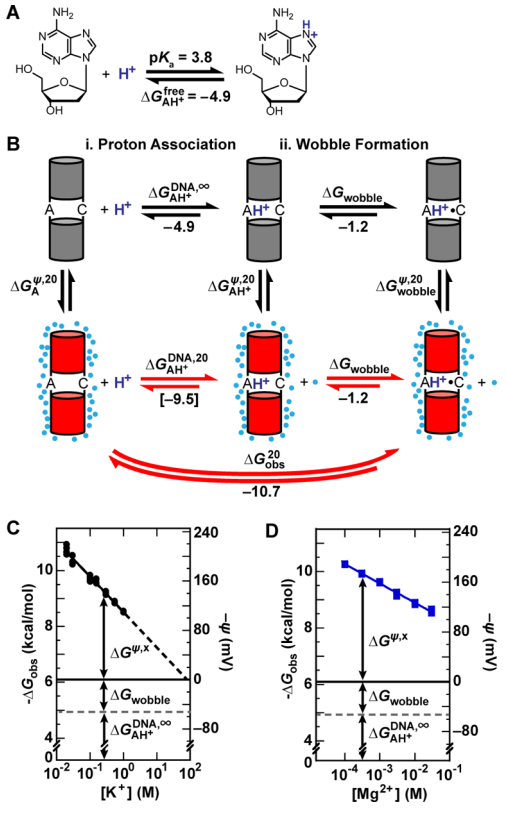

Figure 3. Thermodynamic framework for AH$^+$·C wobble formation within a DNA duplex. Energies are reported as kcal/mol at 25 °C. (A) Protonation of free adenosine, as previously measured,[67] represents the "intrinsic" proton affinity of an A·C mismatch—i.e., proton association without the contributions of the DNA charge and hydrogen bonding. (B) Thermodynamic cycle comparing AH$^+$·C wobble formation without (top) and with (bottom) electrostatic interactions. The top (gray) panel represents the equilibria for a hypothetical state with full screening of electrostatic interactions ([salt] = ∞), and the bottom (red) panel refers to the same equilibria in the presence of 20 mM K$^+$, conditions that give $\Delta G^{20}_{obs} = -10.7$ kcal/mol (Figure 2C and Table S2). For both cases, AH$^+$·C wobble formation includes two steps, proton association (i) and wobble pair formation (ii). In uncharged DNA (gray cylinders), protonation of A is assumed to be equal to the "intrinsic" proton affinity presented in Figure A ($\Delta G^{DNA,\infty}_{AH+} = \Delta G^{free}_{AH+}$). The energetics of wobble formation in the absence of additional electrostatic factors was estimated from measured duplex stabilities and derived nearest neighbor rules for an A·C mismatch versus a neutral G·T wobble (Figure S8).[61,69] The value of $\Delta G^{DNA,20}_{AH+} = -9.5$ kcal/mol was determined from the thermodynamic cycle and the relationship obtained from this cycle: $\Delta G^{DNA,20}_{AH+} = \Delta G^{20}_{obs} - \Delta G_{wobble} = -10.7 - (-1.2)$ kcal/mol. The vertical equilibria represent the energetic changes arising from charging the DNA from a state absent of electrostatic interactions to the 20 mM K$^+$ conditions. The superscript ψ is used because this change is related to the electrostatic potential, as described in the main text. As noted in the text, it is assumed that wobble formation is salt independent (subsequent to protonation), so that $\Delta G^{\psi,20}_{AH+} = \Delta G^{\psi,20}_{wobble}$. (C and D) Electrostatic potential estimates for the proton binding site of 24bp^{AC}. The thermodynamic framework and free energy terms in part B were used to estimate the electrostatic potential at varying concentrations of K$^+$ (C) and Mg^{2+} (D) ($\Delta G^{DNA,x}_{AH+} - \Delta G^{DNA,\infty}_{AH+}$, x = 20−1000 mM K$^+$ or 0.1−30 mM Mg^{2+}). The conversion between free energy and potential is 1 kcal/mol = 45 meV.

acid concentrations, and we speculate that salt brought along with the DNA may have resulted in smaller changes in the total solution salt concentration than reported based on the amount of added salt. Additionally or alternatively, a protonation-coupled folding transition stabilized by salt and a lower electrostatic potential in the short DNA hairpin, attributable to end-effects,[26,27,65,66] could contribute to the lower observed slope.

Estimating the Electrostatic Potential at the Nucleic Acid-Ion Atmosphere Interface. The log K_A (equivalent to pK_a) observed for protonation of the A residue of the A·C mismatch in 24bp^{AC} of ∼6−8 (Figure 2C) was well above the pK_a of 3.8 for deoxyadenosine in solution (Figure 3A).[67] At the lowest salt measured, the observed pK_a of 24bp^{AC} was 8.2, corresponding to a difference of 4.4 pK_a units (= [8.2−3.8]; 20 mM K$^+$; Figure 2C) and a free energy difference of 5.7 kcal/mol. The observation that this attraction is mitigated with increased K$^+$ and more so with Mg^{2+}, as described in the prior section (Figure 2C), strongly supports a polyelectrolyte and electrostatic origin of this effect. Nevertheless, there is a second factor that is also expected to contribute to the observed equilibrium, the conversion of the A·C mismatch to a more stable AH$^+$·C wobble pair (Figure 1C).[42,68] We therefore used a thermodynamic cycle to separate these factors and isolate the contribution of the electrostatic potential to proton affinity.

Figure 3B shows protonation of the A·C mismatch of 24bp^{AC} broken into two steps: i. protonation and ii. formation of the wobble pair. The top row (in gray) represents the hypothetical standard state under conditions with electrostatic screening such that there are no electrostatic effects. Under these conditions, the association of a proton to the A residue simply reflects that of free adenosine in solution, and we therefore assign it the same ΔG value (i.e., $\Delta G^{DNA,\infty}_{AH+} = \Delta G^{free}_{AH+} = -4.9$ kcal/mol; Figure 3A and 3B). Next, we estimated the free energy for converting a mismatch to a wobble pair (ΔG_{wobble}). We use established nearest neighbor parameters for DNA helix stability, comparing values for an A·C mismatch versus a G·T wobble with the neighboring base pairs found in 24bp^{AC} (Figure S8).[61,69] In other words, formation of a G·T wobble was used as a model for formation of the AH$^+$·C wobble in the absence of the additional electrostatic effects from the positive charge of the protonated base.

We can now compare the energetics of protonation at each salt condition to the standard state in the absence of electrostatic effects that is shown in gray in the top row of Figure 3B. The bottom row of Figure 3B (red) shows one such comparison, for 20 mM K$^+$. At 20 mM K$^+$, the observed log K_A value is 8.2, corresponding to $\Delta G^{20}_{obs} = -10.7$ kcal/mol, and we assume that ΔG_{wobble} is independent of salt and therefore the same as the value of −1.2 kcal/mol derived above. Using the thermodynamic cycle of Figure 3B (red), we can solve for $\Delta G^{DNA,20}_{AH+}$ (= $\Delta G^{20}_{obs} - \Delta G_{wobble}$ = [−10.7 − (−1.2) = −9.5 kcal/mol]). With this value in hand, we can compare the proton attraction in the absence of the DNA electrostatic effects ($\Delta G^{DNA,\infty}_{AH+}$, at infinite screening) to that in the presence of 20 mM K$^+$ ($\Delta G^{DNA,20}_{AH+}$). The difference between these values, $\Delta G^{DNA,20}_{AH+} - \Delta G^{DNA,\infty}_{AH+} = -9.5 - (-4.9) = -4.6$ kcal/mol, is the energetic effect of the field present at 20 mM K$^+$ in attracting the proton. Although there are simplifications in the thermodynamic cycles of Figure 3B, including assuming that the energetics for formation of a neutral wobble pair and neutral mismatch have the same salt dependences, the calculated effect is substantial and likely to be much larger than these uncertainties and thus a good estimate of the underlying electrostatic energetics.

Figures 3C and 3D generalize the electrostatic energies to the remainder of the conditions studied herein for K$^+$ and Mg^{2+}, respectively, and the graphical depiction provides an intuitive guide to the parsing of this effect. The bottom dashed line

DOI: 10.1021/jacs.7b01830
J. Am. Chem. Soc. 2017, 139, 7540−7548

represents the energetics for protonation of adenosine ($\Delta G^{DNA,\infty}_{AH+}$) in the absence of electrostatic effects (Figure 3B), and the favorable effect for forming a wobble pair, ΔG_{wobble}, is represented by the next double-headed arrow and gives a combined value of ΔG_{obs} = −6.1 kcal/mol (Figures 3C and D, solid lines); this value is the proton affinity expected in the absence of any favorable electrostatics effects. The observed free energy values are well beyond this estimated baseline across the entire range of K^+ and Mg^{2+} concentrations investigated, providing strong evidence for a considerable electrostatic contribution to proton binding even at 1 M monovalent salt, the highest concentration investigated herein. This experimental result is in contrast to a common literature statement that the free energies of association in 1 M salt represent nonelectrostatic contributions.[8,23,25,70−72]

The electrostatic energies derived above can be expressed in terms of the potential that is felt by the attracted proton, an important conversion as polyelectrolytes are often described in terms of electrostatic potentials that diminish with distance from the molecule. As our protonation occurs on a base, the electrostatic potential is expected to reflect that at or near to the nucleic acid surface. PB theory predicts values of −200 to −300 mV across the range of salt concentrations investigated herein (Figure S5), and these predicted values can be compared to those determined herein.

To obtain the electrostatic potential we used the standard equation relating it to free energy (eq 7),[73,74] and we used the free energy "excess" over that predicted for the proton affinity of the adenosine residue ($\Delta G^{DNA,\infty}_{AH+}$ = −4.9 kcal/mol) and formation of the wobble (ΔG_{wobble} = −1.2 kcal/mol); this baseline is represented by the solid lines in Figures 3C and D at $-\Delta G_{obs}$ = 6.1 kcal/mol, as noted above. The electrostatic potentials calculated from the excess free energy and eq 7 are plotted on the right axes in Figures 3C and 3D as a function of K^+ and Mg^{2+} concentration, respectively. These values are within the range estimated from PB theory (Figure S5) and indeed are in reasonable agreement, especially considering the mean-field nature of PB theory and the difficulty of defining an exact protonation position (Figure S5G). Overall, these results suggest that the AH^+·C wobble system can be used as an empirical electrostatic meter than can be incorporated with minimal perturbation into a range of nucleic acid systems.

Organization of the Ion Atmosphere Probed with Ligand Association in Mixed Divalent/Monovalent Salt Solutions. We used the distinct effects of Mg^{2+} and K^+ to further characterize the proton association properties of $24bp^{AC}$, to test additional predictions from polyelectrolyte theory, and to explore properties of the ion atmosphere.

The Mg^{2+} concentration dependence shown in Figure 2C was carried out with a background of 20 mM K^+. We reasoned that with a sufficiently higher background of K^+ ion, the initial Mg^{2+} added would not outcompete K^+ for occupancy of the ion atmosphere and would thus have no effect on proton affinity (K_A). Conversely, at a sufficiently high concentration of Mg^{2+} in the higher K^+ background, Mg^{2+} would preferentially occupy the ion atmosphere. At this point, the K_A values should be the same as that in the lower K^+ background and the Mg^{2+} concentration dependencies should superimpose. Indeed, earlier PB calculations by Honig and Draper predicted such a change in slope, from conditions for which Mg^{2+} has no effect to conditions for which it is dominant.[59,63,75]

Figure 4A shows that the observed behavior follows this prediction and is indicative of competition between K^+ and Mg^{2+}

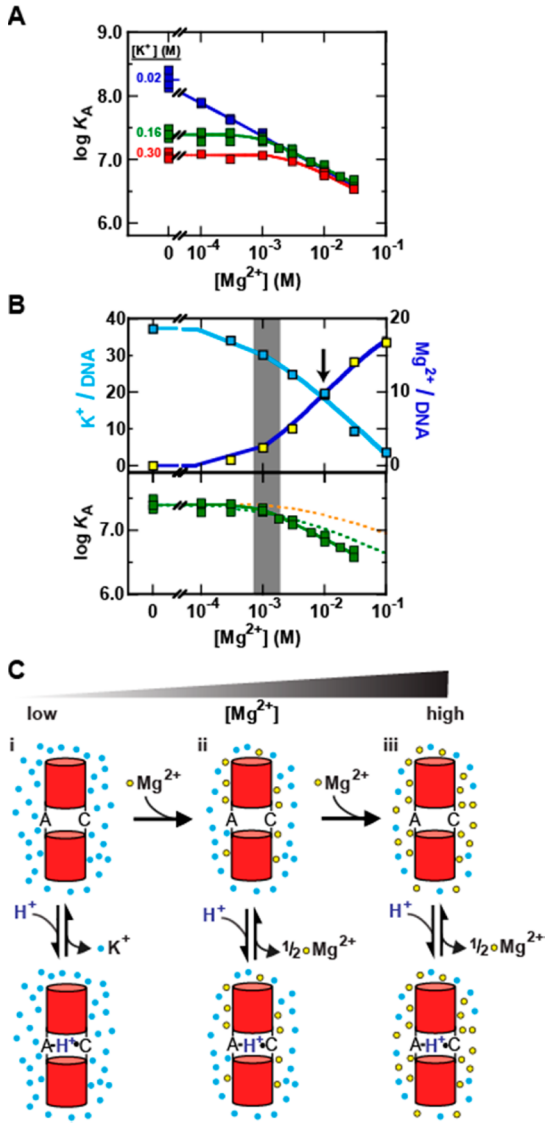

Figure 4. Probing ion atmosphere properties via proton association in mixed divalent/monovalent cation solutions. (A) Observed proton association constants (K_A) for a range of Mg^{2+} concentrations in K^+ backgrounds of 20 mM (blue), 160 mM (green), and 300 mM (red). (B) Comparison of the composition of the ion atmosphere, as determined by ion counting (top panel: K^+ (160 mM) light blue; Mg^{2+} (varied), dark blue) to the Mg^{2+} dependence of the proton association (log K_A, bottom panel, also with 160 mM K^+). The gray box denotes the concentration region where log K_A transition from having no Mg^{2+} dependence (slope = 0) to the full Mg^{2+} dependence (slope ∼ −0.5). The Mg^{2+} concentration dependence of proton association predicted by a stochastic cation release model is shown by the dashed orange line. The PB-predicted Mg^{2+} dependence of proton association is shown with the green dashed line. (C) Schematic representation of monovalent and divalent cation release upon proton binding. (i) Ion atmosphere saturated with monovalent cation, K^+, and K^+ is primarily released upon proton binding. (ii) With a small amount of Mg^{2+} in the ion atmosphere, the Mg^{2+} ions preferentially associate close to DNA, and proton binding at the interface of the DNA/ion atmosphere is predominantly accompanied by release of 0.5 Mg^{2+} ions, despite their underrepresentation in the atmosphere relative to K^+. (iii) Further Mg^{2+} titration leads to complete K^+ replacement, with the more distal K^+ ions replaced last, on average.

for the ion atmosphere. With a background of 160 mM K^+, added Mg^{2+} up to ∼1 mM had no effect—i.e., the slope is zero (green

DOI: 10.1021/jacs.7b01830
J. Am. Chem. Soc. 2017, 139, 7540−7548

points and line). Nevertheless, at higher Mg^{2+} concentrations this curve meets and then follows the analogous low K^+ background curve (blue points and line). Analogous behavior was observed in a background of 300 mM K^+, but higher Mg^{2+} concentrations were needed to begin to affect the proton affinity (red points and line), as expected due to competition.

To compare the transition in Figure 4A from Mg^{2+}-independent to Mg^{2+}-dependent behavior to the actual occupancy of the ion atmosphere we carried out ion counting with the DNA duplex used in this study, though with the 2AP residue replaced by A. With a background of 160 mM K^+ we equilibrated with a series of Mg^{2+} concentrations and at each concentration used inductively coupled plasma optical emission spectrometry (ICP-OES) to "count" the excess number of K^+ and Mg^{2+} ions in the ion atmosphere of the DNA duplex.[48,49] The Mg^{2+} concentration needed to displace half of the K^+ was ~10 mM (Figure 4B, arrow), giving a ratio of ~16, relative to the background 160 mM K^+. This ratio is consistent with ion competition results with other DNA duplexes of 10−20.[33] However, the proton affinity (log K_A) responded at much lower Mg^{2+} concentrations, with the change from zero slope to the Mg^{2+}-dependent slope of −0.5 occurring at ~1 mM Mg^{2+} (Figure 4B, gray bar).

To evaluate this differential effect, we created a null stochastic model in which the ion atmosphere adjustment upon A·C protonation (to give the AH^+·C wobble) is equally likely to arise from expulsion of Mg^{2+} (one-half) or K^+, based simply on the abundance of each ion in the atmosphere. This stochastic model predicts a smooth transition from slope 0 to slope −0.5 that mirrors the K^+ displacement from the ion atmosphere as the Mg^{2+} concentration is increased (Figure 4B, orange dashed curve). Instead, Mg^{2+} is preferentially expelled from the ion atmosphere at lower Mg^{2+} concentrations (Figure 4B, squares).

The ion counting results indicate that there are, on average, only ~2−4 Mg^{2+} ions in the ion atmosphere, in comparison to ~28−32 K^+ ions, when loss of Mg^{2+} becomes dominant upon protonation—i.e., when the slope changes from zero to −0.5 (Figure 4B, gray box). What could cause such a preference? The first Mg^{2+} ions to enter the ion atmosphere are expected to preferentially localize close to the DNA duplex, driven by the stronger electrostatic attraction and lower entropic cost for localization of one divalent over two monovalent cations; these cations may correspond to "tightly bound" ions proposed in several models.[6,76−78] Our results suggest that the protonation occurs essentially at the DNA/ion atmosphere interface and preferentially induces loss of Mg^{2+} from the tightly bound layer (Figure 4C). Thus, our results provide experimental support for the predicted differential positioning of divalent and monovalent cations within an ion atmosphere.

CONCLUSIONS AND IMPLICATIONS

While electrostatics is a ubiquitous force in nucleic acid folding, recognition, and function, it has been difficult to address experimentally. In part, this difficulty stems from the dynamic nature of the ion atmosphere that surrounds nucleic acids and other polyelectrolytes, which blunts the power of standard molecular biology tool such as structure determination. Correspondingly, theoretical approaches have been prevalent in evaluating polyelectrolytes; however, their value can only be established via independent experimental tests.[79−81] Recent ion counting studies, which provide a thermodynamic determination of the ion atmosphere content, contradict the common finding from computational studies of size-dependent ion atmosphere occupancy by cations.[64] There is a dire need for additional experimental measurements of nucleic acid electrostatics and ion atmosphere behavior to provide a foundation for next-generation theory and computation.

Experimentally, electrostatic effects arise in most, if not all, nucleic acid studies. However, the complexity of most biological systems precludes isolating and quantifying these effects. Correspondingly, simple, defined systems, often of nonbiological origin, have provided the most fertile ground for interrogating electrostatic behaviors of nucleic acids and their ion atmosphere, for revealing foundational properties, and for testing electrostatic theories.[2,75,82,83] For example, studies of defined DNA duplexes allowed quantitation of the ion atmosphere contents and studies of DNA duplexes connected by flexible PEG tethers provided evidence for a lessening of repulsive electrostatic forces and a corresponding conformational relaxation upon Mg^{2+} addition, rather than Mg^{2+}-induced attractive forces.[84,85]

While systematic studies of properties of simple nucleic acid systems, especially their ion atmospheres, have provided much needed information,[48,49,64,86−88] it has been considerably more difficult to quantitatively probe electrostatic interaction energies. With this motivation, we turned to a clever system developed by Bevilacqua and co-workers involving protonation of an A·C mismatch within a DNA helix to form an AH^+·C wobble pair (Figure 1C). Using this system, we were able to test predictions from polyelectrolyte theories, obtain information pertinent to nucleic acid-ligand association studies, and measure local electrostatic energies and potentials.

Our results provide strong support for general ion atmosphere properties predicted by polyelectrolyte theories. These conclusions are consistent with conclusions from previous ligand association studies that measured salt-dependences of Mg^{2+}, polyamine, and oligopeptide association but required simplifications in the analyses linking the results and theories.[5,8,17−29] As predicted by polyelectrolyte theories, association of a proton ligand with a DNA helix resulted predominantly in a loss of an ion atmosphere cation, rather than uptake of an anion (Figure 2). The observed preferential loss of Mg^{2+} rather than K^+ in mixed salt solutions is also predicted by polyelectrolyte theory (Figure 4B, green solid vs dashed lines). These data also revealed an asymmetry in the release of divalent and monovalent cations from the ion atmosphere upon A·C protonation, consistent with the predicted preferential occupancy of divalent cations over monovalents proximal to the polyelectrolyte (Figure 4C).

Several studies have reported salt dependences at odds with expectations from polyelectrolyte theory.[41,30−32,42,33] Prior paradoxical salt dependences may have arisen from incomplete accounting of background ions, titration effects that cause miscalculation of the free cation concentration, complications from transition regions in mixed solutions of monovalent and divalent cations (Figure 4A), and conformational changes coupled to association. It has been suggested that salt concentration dependences for protein binding to DNA and RNA allow determination of the number of ion pairs in the bound complex.[16,30−37] However, this correspondence was based on ad hoc definitions of ion pairs, based on a consistency with experiment in the absence of independent experimental tests. Limitations of this treatment have been noted.[38−40] Our studies pave the way for careful dissection of more complex systems to deepen understanding of the electrostatics that underlie nucleic acid-ligand interactions.

Our results underscore the substantial energetics associated with electrostatics for nucleic acid systems and suggest caution in

DOI: 10.1021/jacs.7b01830
J. Am. Chem. Soc. 2017, 139, 7540−7548

accepting results and conclusions from calculations and simulations that use simplifications such as including only sufficient salt to neutralize the nucleic acid charge or turning charges off.

Finally and excitingly, we provide experimental evidence that the proton binding to AH^+·C wobble pair serves as a local potential meter at the DNA/ion atmosphere interface (Figure 3B). As predicted by theory, measured potentials attenuate with increasing salt concentration and respond to differences in ion valences. Further, the estimated magnitudes of the electrostatic potential at the DNA/ion atmosphere interface agree well with the theory (Figure 3C and Figure S5G). These findings and the AH^+·C wobble system will provide new opportunities to dissect and understand nucleic acid and nucleic acid/protein complex electrostatic properties and energetics.

■ ASSOCIATED CONTENT

Supporting Information

The Supporting Information is available free of charge on the ACS Publications website at DOI: 10.1021/jacs.7b01830.

Figures S1−S8, Tables S1−S7, Methods (PDF)

■ AUTHOR INFORMATION

Corresponding Author

*herschla@stanford.edu

ORCID

Benjamin E. Allred: 0000-0003-2562-4496

Notes

The authors declare no competing financial interest.

■ ACKNOWLEDGMENTS

We thank members of the Herschlag lab and Jan Lipfert for helpful discussions and advice. This work was supported by the National Institutes of Health (grant P01GM066275 to D.H.).

■ REFERENCES

(1) Draper, D. E.; Grilley, D.; Soto, A. M. *Annu. Rev. Biophys. Biomol. Struct.* **2005**, *34* (1), 221.
(2) Chu, V. B.; Bai, Y.; Lipfert, J.; Herschlag, D.; Doniach, S. *Curr. Opin. Chem. Biol.* **2008**, *12* (6), 619.
(3) Lipfert, J.; Doniach, S.; Das, R.; Herschlag, D. *Annu. Rev. Biochem.* **2014**, *83* (1), 813.
(4) Latt, S. A.; Sober, H. A. *Biochemistry* **1967**, *6* (10), 3293.
(5) Record, M. T.; Anderson, C. F.; Lohman, T. M. *Q. Rev. Biophys.* **1978**, *11* (2), 103.
(6) Manning, G. S. *Q. Rev. Biophys.* **1978**, *11* (2), 179.
(7) Manning, G. S. *J. Chem. Phys.* **1969**, *51* (3), 924.
(8) Record, M. T.; Lohman, T. M.; Haseth, P. de. *J. Mol. Biol.* **1976**, *107* (2), 145.
(9) Jayaram, B.; Sharp, K. A.; Honig, B. *Biopolymers* **1989**, *28* (5), 975.
(10) Sharp, K. A.; Honig, B.; Harvey, S. C. *Biochemistry* **1990**, *29* (2), 340.
(11) Sharp, K. A.; Honig, B. *J. Phys. Chem.* **1990**, *94* (19), 7684.
(12) Stigter, D.; Dill, K. A. *Biophys. J.* **1996**, *71* (4), 2064.
(13) Baker, N. A.; Sept, D.; Joseph, S.; Holst, M. J.; McCammon, J. A. *Proc. Natl. Acad. Sci. U. S. A.* **2001**, *98* (18), 10037.
(14) Unni, S.; Huang, Y.; Hanson, R. M.; Tobias, M.; Krishnan, S.; Li, W. W.; Nielsen, J. E.; Baker, N. A. *J. Comput. Chem.* **2011**, *32* (7), 1488.
(15) Misra, V. K.; Sharp, K. A.; Friedman, R. A.; Honig, B. *J. Mol. Biol.* **1994**, *238* (2), 245.
(16) DeHaseth, P. L.; Lohman, T. M.; Record, M. T. *Biochemistry* **1977**, *16* (22), 4783.
(17) Mascotti, D. P.; Lohman, T. M. *Proc. Natl. Acad. Sci. U. S. A.* **1990**, *87* (8), 3142.
(18) Wilson, W. D.; Krishnamoorthy, C. R.; Wang, Y.-H.; Smith, J. C. *Biopolymers* **1985**, *24* (10), 1941.
(19) Jones, R. L.; Wilson, W. D. *Biopolymers* **1981**, *20* (1), 141.
(20) Breslauer, K. J.; Remeta, D. P.; Chou, W. Y.; Ferrante, R.; Curry, J.; Zaunczkowski, D.; Snyder, J. G.; Marky, L. A. *Proc. Natl. Acad. Sci. U. S. A.* **1987**, *84* (24), 8922.
(21) Chaires, J. B.; Satyanarayana, S.; Suh, D.; Fokt, I.; Przewloka, T.; Priebe, W. *Biochemistry* **1996**, *35* (7), 2047.
(22) Wang, S.; Kumar, A.; Aston, K.; Nguyen, B.; Bashkin, J. K.; Boykin, D. W.; Wilson, W. D. *Chem. Commun.* **2013**, *49* (76), 8543.
(23) Mascotti, D. P.; Lohman, T. M. *Biochemistry* **1992**, *31* (37), 8932.
(24) Mascotti, D. P.; Lohman, T. M. *Biochemistry* **1993**, *32* (40), 10568.
(25) Mascotti, D. P.; Lohman, T. M. *Biochemistry* **1997**, *36* (23), 7272.
(26) Zhang, W.; Bond, J. P.; Anderson, C. F.; Lohman, T. M.; Record, M. T. *Proc. Natl. Acad. Sci. U. S. A.* **1996**, *93* (6), 2511.
(27) Zhang, W.; Ni, H.; Capp, M. W.; Anderson, C. F.; Lohman, T. M.; Record, M. T., Jr. *Biophys. J.* **1999**, *76* (2), 1008.
(28) Braunlin, W. H.; Strick, T. J.; Record, M. T. *Biopolymers* **1982**, *21* (7), 1301.
(29) Olmsted, M. C.; Bond, J. P.; Anderson, C. F.; Record, M. T. *Biophys. J.* **1995**, *68* (2), 634.
(30) Winter, R. B.; Von Hippel, P. H. *Biochemistry* **1981**, *20* (24), 6948.
(31) Jen-Jacobson, L.; Kurpiewski, M.; Lesser, D.; Grable, J.; Boyer, H. W.; Rosenberg, J. M.; Greene, P. J. *J. Biol. Chem.* **1983**, *258* (23), 14638.
(32) Hall, K. B.; Stump, W. T. *Nucleic Acids Res.* **1992**, *20* (16), 4283.
(33) Romaniuk, P. J. *Nucleic Acids Res.* **1985**, *13* (14), 5369.
(34) Barkley, M. D.; Lewis, P. A.; Sullivan, G. E. *Biochemistry* **1981**, *20* (13), 3842.
(35) Takahashi, M.; Blazy, B.; Baudras, A. *Nucleic Acids Res.* **1979**, *7* (6), 1699.
(36) Koh, J.; Shkel, I.; Saecker, R. M.; Record, M. T. *J. Mol. Biol.* **2011**, *410* (2), 241.
(37) Kalodimos, C. G.; Biris, N.; Bonvin, A. M. J. J.; Levandoski, M. M.; Guennuegues, M.; Boelens, R.; Kaptein, R. *Science* **2004**, *305* (5682), 386.
(38) Sharp, K. A.; Friedman, R. A.; Misra, V.; Hecht, J.; Honig, B. *Biopolymers* **1995**, *36* (2), 245.
(39) Fenley, M. O.; Russo, C.; Manning, G. S. *J. Phys. Chem. B* **2011**, *115* (32), 9864.
(40) García-García, C.; Draper, D. E. *J. Mol. Biol.* **2003**, *331* (1), 75.
(41) Halford, S. E.; Johnson, N. P. *Biochem. J.* **1980**, *191* (2), 593.
(42) Siegfried, N. A.; O'Hare, B.; Bevilacqua, P. C. *Biochemistry* **2010**, *49* (15), 3225.
(43) Wilcox, J. L.; Bevilacqua, P. C. *J. Am. Chem. Soc.* **2013**, *135* (20), 7390.
(44) Wilcox, J. L.; Bevilacqua, P. C. *Biochemistry* **2013**, *52* (42), 7470.
(45) Shimizu, T.; Toumoto, A.; Ihara, K.; Shimizu, M.; Kyogoku, Y.; Ogawa, N.; Oshima, Y.; Hakoshima, T. *EMBO J.* **1997**, *16* (15), 4689.
(46) Dolinsky, T. J.; Nielsen, J. E.; McCammon, J. A.; Baker, N. A. *Nucleic Acids Res.* **2004**, *32* (Suppl. 2), W665.
(47) Dolinsky, T. J.; Czodrowski, P.; Li, H.; Nielsen, J. E.; Jensen, J. H.; Klebe, G.; Baker, N. A. *Nucleic Acids Res.* **2007**, *35* (Suppl. 2), W522.
(48) Bai, Y.; Greenfeld, M.; Travers, K. J.; Chu, V. B.; Lipfert, J.; Doniach, S.; Herschlag, D. *J. Am. Chem. Soc.* **2007**, *129* (48), 14981.
(49) Gebala, M.; Giambaşu, G. M.; Lipfert, J.; Bisaria, N.; Bonilla, S.; Li, G.; York, D. M.; Herschlag, D. *J. Am. Chem. Soc.* **2015**, *137* (46), 14705.
(50) Davies, C. W. *Ion Association*; Butterworths: London, 1962.
(51) Zheng, G.; Lu, X.-J.; Olson, W. K. *Nucleic Acids Res.* **2009**, *37* (Suppl. 2), W240.
(52) Hunter, W. N.; Brown, T.; Kennard, O. *Nucleic Acids Res.* **1987**, *15* (16), 6589.
(53) Tang, C. L.; Alexov, E.; Pyle, A. M.; Honig, B. *J. Mol. Biol.* **2007**, *366* (5), 1475.
(54) Robinson, R. A.; Stokes, R. H. *Electrolyte Solutions*, 2nd rev. ed.; Dover Publications: Mineola, NY, 2002.
(55) Kotin, L.; Nagasawa, M. *J. Chem. Phys.* **1962**, *36* (4), 873.
(56) Gross, L. M.; Strauss, U. P. In *Chemical Physics of Ionic Solutions*; Conway, B. E., Barradas, R. G., Eds.; Wiley: New York, 1966; p 295.

DOI: 10.1021/jacs.7b01830
J. Am. Chem. Soc. 2017, 139, 7540−7548

(57) Stigter, D. *J. Colloid Interface Sci.* **1975**, *53* (2), 296.
(58) Sharp, K. A. *Biopolymers* **1995**, *36* (2), 227.
(59) Misra, V. K.; Draper, D. E. *J. Mol. Biol.* **1999**, *294* (5), 1135.
(60) Allawi, H. T.; SantaLucia, J. *Nucleic Acids Res.* **1998**, *26* (21), 4925.
(61) Allawi, H. T.; SantaLucia, J. *Biochemistry* **1998**, *37* (26), 9435.
(62) Peyret, N.; Seneviratne, P. A.; Allawi, H. T.; SantaLucia, J. *Biochemistry* **1999**, *38* (12), 3468.
(63) Chen, S. W.; Honig, B. *J. Phys. Chem. B* **1997**, *101* (44), 9113.
(64) Gebala, M.; Bonilla, S.; Bisaria, N.; Herschlag, D. *J. Am. Chem. Soc.* **2016**, *138* (34), 10925.
(65) Ballin, J. D.; Shkel, I. A.; Record, M. T. *Nucleic Acids Res.* **2004**, *32* (11), 3271.
(66) Shkel, I. A.; Ballin, J. D.; Record, M. T. *Biochemistry* **2006**, *45* (27), 8411.
(67) Izatt, R. M.; Christensen, J. J.; Rytting, J. H. *Chem. Rev.* **1971**, *71* (5), 439.
(68) Moody, E. M.; Lecomte, J. T. J.; Bevilacqua, P. C. *RNA* **2005**, *11* (2), 157.
(69) Allawi, H. T.; SantaLucia, J. *Biochemistry* **1997**, *36* (34), 10581.
(70) Privalov, P. L.; Dragan, A. I.; Crane-Robinson, C. *Nucleic Acids Res.* **2011**, *39* (7), 2483.
(71) Lohman, T. M.; DeHaseth, P. L.; Record, M. T. *Biochemistry* **1980**, *19* (15), 3522.
(72) Lohman, T. M.; Mascotti, D. P. *Methods Enzymol.* **1992**, *212*, 400.
(73) Friedrich, K.; Woolley, P. *Eur. J. Biochem.* **1988**, *173* (1), 227.
(74) Dill, K. A.; Bromberg, S. *Molecular Driving Forces*, 2nd ed.; Garland Science: New York, 2010.
(75) Leipply, D.; Draper, D. E. *J. Am. Chem. Soc.* **2011**, *133* (34), 13397.
(76) Murthy, C. S.; Bacquet, R. J.; Rossky, P. J. *J. Phys. Chem.* **1985**, *89* (4), 701.
(77) Tan, Z.-J.; Chen, S.-J. *J. Chem. Phys.* **2005**, *122* (4), 44903.
(78) Yoo, J.; Aksimentiev, A. *J. Phys. Chem. B* **2012**, *116* (43), 12946.
(79) Hempel, C. G. *Philosophy of Natural Science*; Prentice-Hall: Englewood Cliffs, NJ, 1966.
(80) Popper, K. R. *The Logic of Scientific Discovery*, rev. ed.; Harper & Row: New York, 1968.
(81) Popper, K. R. *Realism and the Aim of Science*; Rowman and Littlefield: Totowa, NJ, 1983.
(82) Pollack, L. *Annu. Rev. Biophys.* **2011**, *40*, 225.
(83) Chen, S.-J. *Annu. Rev. Biophys.* **2008**, *37*, 197.
(84) Bai, Y.; Chu, V. B.; Lipfert, J.; Pande, V. S.; Herschlag, D.; Doniach, S. *J. Am. Chem. Soc.* **2008**, *130* (37), 12334.
(85) Bai, Y.; Das, R.; Millett, I. S.; Herschlag, D.; Doniach, S. *Proc. Natl. Acad. Sci. U. S. A.* **2005**, *102* (4), 1035.
(86) Pabit, S. A.; Meisburger, S. P.; Li, L.; Blose, J. M.; Jones, C. D.; Pollack, L. *J. Am. Chem. Soc.* **2010**, *132* (46), 16334.
(87) Andresen, K.; Das, R.; Park, H. Y.; Smith, H.; Kwok, L. W.; Lamb, J. S.; Kirkland, E. J.; Herschlag, D.; Finkelstein, K. D.; Pollack, L. *Phys. Rev. Lett.* **2004**, *93* (24), 248103.
(88) Meisburger, S. P.; Pabit, S. A.; Pollack, L. *Biophys. J.* **2015**, *108* (12), 2886.

DOI: 10.1021/jacs.7b01830
J. Am. Chem. Soc. 2017, 139, 7540−7548